Sustainability in Environment
ISSN 2470-637X (Print) ISSN 2470-6388 (Online)
Vol. 11, No. 2, 2026
www.scholink.org/ojs/index.php/se

Original Paper

Characteristics and Meteorological Mechanisms of Typical Nocturnal Ozone Increase Events in Suizhou, China

Ge Li[1,2] & Zhenxin Liu[1*]

[1] School of Environmental Science and Engineering, Nanjing University of Information Science and Technology, Nanjing, Jiangsu, China

[2] Suizhou Meteorological Bureau, Hubei, China

[*] Corresponding Author

Received: February 29, 2026 Accepted: April 27, 2026 Online Published: May 14, 2026

doi:10.22158/se.v12n1p340 URL: http://dx.doi.org/10.22158/se.v12n1p340

Abstract

In recent years, ozone pollution has become increasingly prominent in China. Surface ozone not only rises during the daytime but also exhibits secondary increases at night, defined as nighttime ozone increase events (NOIs). Using atmospheric pollutant concentration data from 2015 to 2023, this study analyzes the characteristics of NOIs in Suizhou, including their frequency, intensity, and nocturnal and daytime peak concentrations. The WRF-Chem model is also employed to simulate the event with the maximum intensity. The results show that a total of 614 NOIs occurred in Suizhou, accounting for 18.7% of the total observation period. The maximum intensity of these events reached 57 μg/(m³·h). In 12.2% of the NOIs, the nocturnal ozone peak (NOP) exceeded the previous daytime maximum (PDM), indicating that NOIs in Suizhou cannot be ignored. The simulation results indicate that large-scale subsidence transports ozone-rich air from the upper layers downward, while horizontal advection carries high-concentration ozone from northeastern Hubei Province to Suizhou. Furthermore, the drag effect of precipitation particles and turbulent disturbances following the initiation of nighttime convection further bring residual layer ozone to the surface. Collectively, these processes lead to the increase in nocturnal surface ozone concentrations.

Keywords

Suizhou, nighttime ozone increase (NOIs), WRF-Chem

1. Introduction

In recent years, surface ozone pollution has become increasingly prominent in China, especially in summer when ozone has become the primary factor causing air quality exceedances in some cities.

Previous studies have shown that ozone, as a secondary pollutant, is mainly produced by photochemical reactions involving anthropogenic and natural emissions of nitrogen oxides (NOx), carbon monoxide (CO), and volatile organic compounds (VOCs) under solar radiation (Wang et al., 2012; An et al., 2024). At night, surface ozone concentrations generally decrease due to NOx titration and dry deposition (Brown et al., 2006). Given the current emission status of ozone precursors in the lower atmosphere and the mechanisms of ozone formation, surface ozone concentrations typically peak during the daytime and reach a minimum around 06:00 LT the next day (Cheng et al., 2016; Li et al., 2019). Both observations and simulations have found that ozone concentrations in most Chinese cities exhibit a unimodal diurnal pattern characterized by high daytime and low nighttime values (An et al., 2007; Wang et al., 2018), which is also a typical feature of the surface ozone diurnal cycle. However, influenced by weather or other factors, frequent observations in recent years have revealed a bimodal diurnal pattern of surface ozone, with ozone concentrations unexpectedly increasing at night (Kulkarni, Bortoli, Silva, & Reeves, 2015; Kalthoff et al., 2000; Zhang 1998; He et al., 2022), defined as nighttime ozone increase events (NOIs). Up to now, NOIs have been observed worldwide, indicating their global universality.

The occurrence of NOIs not only alters the ozone diurnal cycle but may also increase the exposure time of humans, animals, and plants to ozone. Research results show that a 10 ppbv increase in ozone concentration is associated with a 0.3% increase in mortality, and even relatively low ozone levels can lead to an increased risk of premature death, threatening human health and affecting crop yields (Feng et al., 2022). From an agricultural perspective, when nocturnal ozone concentrations exceed 80 $\mu g/m^3$, they can cause plant water loss and yield reduction (Zhu et al., 2024); when nocturnal ozone concentrations exceed 45 ppb (approximately 90 $\mu g/m^3$), yield losses of sensitive crop varieties can reach 15% (Lloyd, Davis, Marini, & Decoteau, 2020). Furthermore, the increase in nocturnal ozone strengthens the absorption of longwave radiation from the ground, causing local temperature changes and thus affecting the accuracy of temperature forecasts (Kulkarni, Bortoli, & Silva, 2013).

Previous studies on ozone have mostly focused on daytime ozone pollution events, including their spatiotemporal distribution characteristics, influence mechanisms, and source apportionment (Yan et al., 2020; Yan et al., 2019). In recent years, although attention to nocturnal ozone has gradually increased, research on NOIs in China has mainly concentrated in densely populated city clusters such as the North China Plain, the Yangtze River Delta, and the Pearl River Delta (He et al., 2022; Zhu et al., 2020; Wu et al., 2023), while studies on NOIs in Hubei Province remain relatively limited. Suizhou (112.43°E-114.07°E, 31.19°N-32.26°N) is an important city in northern Hubei, located at the intersection of the Yangtze River Basin and the Huaihe River Basin. It has been rated as an ecologically livable city, and its air quality has drawn considerable attention. Current research on ozone in Suizhou has mainly focused on characteristic analysis, relationships with meteorological factors, and pollution causes (Chen et al., 2020; Chen et al., 2017; Yang et al., 2025; Xu et al., 2025; Wu et al., 2024)[24-28]; however, no systematic study has yet been conducted on NOIs in Suizhou. Therefore, this study

investigates the statistical characteristics of NOIs in Suizhou from 2019 to 2023, selects the event with the maximum intensity as a typical case, and simulates it using the WRF-Chem model to further explore the impact of meteorological mechanisms on the occurrence and development of NOIs. This work provides new insights into the evolution mechanisms of surface ozone, and is of great significance for improving the forecasting and early warning capabilities of meteorological forecasters and other technical professionals in environmental meteorology, enhancing public and decision-making services, and promoting the development of ecological meteorological services in central China.

2. Data and Methods

2.1 Study Area

Suizhou (112.43°E-114.07°E, 31.19°N-32.26°N) is located in northern Hubei Province (Fig. 1), with an average elevation of approximately 200 meters. The Tongbai Mountains lie to the north, the Dahong Mountain to the southwest, and the western extension of the Dabie Mountains to the east, forming a topographical pattern of three mountains enclosing a corridor. The southeastern plain of Suizhou serves as a key transport pathway for pollutants from North China to the Jianghan Plain.

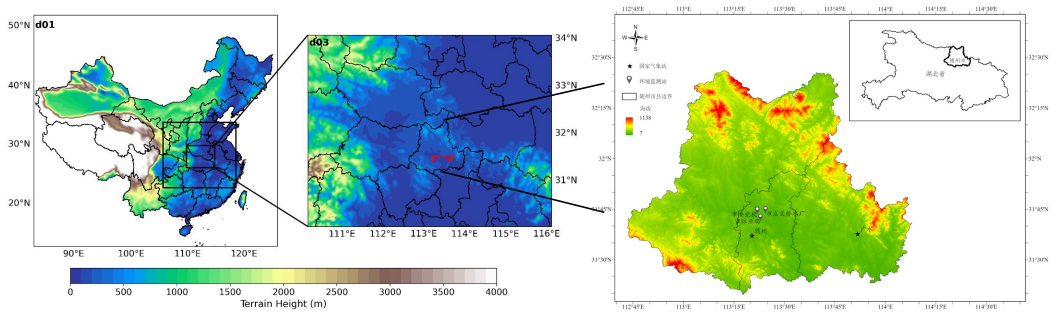

Figure 1. WRF-Chem Model Simulation Domains with three Nested Domains (d01, d02, d03), along with the Topography of Suizhou and the Distribution of Air Quality Monitoring and Meteorological Stations

2.2 Data

(1) Air quality data were obtained from the Hubei Provincial Environmental Monitoring Center Station (http://59.172.208.250:8100/), covering the period from January 1, 2015 to December 31, 2023. The dataset includes hourly data from three national control stations in Suizhou: the Municipal Forestry Bureau (Shi Linyeju), the Municipal Party School (Shiwei Dangxiao), and the Overpass Water Plant (Shiliqiao Shuichang). Referring to the definition of nocturnal ozone increase events in previous studies (Zhu et al., 2024; Wu et al., 2023), a day is identified as having a nighttime ozone increase event (NOIs) if the increase in hourly ozone concentration between two adjacent hours during the nighttime period (20:00 BJT to 06:00 BJT the next day) exceeds 10 μg/m³. If multiple hourly increases exceeding 10 μg/m³ occur on the same night, the night is still counted as only one NOIs. The corresponding

maximum hourly ozone concentration during the night is defined as the nocturnal ozone peak (NOP), while the maximum hourly ozone concentration during the daytime of the same day is defined as the peak daytime maximum (PDM). The hourly ozone increase ($\Delta O_3/\Delta t$) between adjacent nighttime hours is taken as the intensity of the corresponding NOIs.(2) Meteorological data were obtained from the National Meteorological Information Center (http://data.cma.cn/), including surface observations of hourly temperature, precipitation, relative humidity, visibility, and 10-minute average wind speed and direction.

2.3 WRF-Chem Model Configuration

In this study, the WRF-Chem model version 4.6.0 is used to numerically simulate the atmospheric pollution processes in the study area. The model uses the Lambert conformal conical projection for horizontal mapping, with three two-way nested domains at horizontal resolutions of 27 km, 9 km, and 3 km (Fig.1). Vertically, the model adopts a σ-pressure hybrid coordinate system with 38 vertical layers, and the model top is set at 5 hPa. The meteorological initial and boundary conditions are derived from the ERA5 reanalysis dataset, which has a horizontal spatial resolution of 0.25° × 0.25°, a temporal resolution of 1 hour, and includes 38 pressure levels between 1000 hPa and 5 hPa in the vertical direction.

3. Results and Discussion

3.1 Characteristics of NOIs

Based on the analysis of the average ozone concentrations at the three national control stations in Suizhou from 2015 to 2023, a total of 614 NOIs occurred in the city, accounting for 18.7% of the observation period (Fig. 2(a)). Significant seasonal differences were observed over the nine years, with the frequency ranking as summer > autumn > spring > winter, which is consistent with the seasonal variation of daytime ozone concentrations reported in previous studies, typically characterized by high values in summer and low values in winter (Zhang, Q. Q., & Zhang, X. Y., 2019). From the perspective of diurnal variation in frequency (Fig.2(d)), NOIs showed distinct differences during the night. The highest frequency before midnight occurred at 21:00 LT (76 days), while after midnight the highest frequency occurred at 02:00 LT (73 days), and the lowest frequency occurred at 03:00 LT (49 days). Overall, more than half of the NOIs (67%) occurred after midnight, which is consistent with the findings of Zhu et al. [23]. In terms of event intensity (Fig. 2(b)), the ranking was summer > spring > autumn > winter. Summer not only had the highest frequency of NOIs but also the greatest intensity, warranting particular attention. For all seasons, the mean intensity was higher than the median, indicating that weak events were prevalent. The maximum intensity reached 57.0 μg/(m3·h), which occurred on July 14, 2015.

Regarding the relationship between NOP and PDM (Fig.2(c), (d), (e)), the seasonal order of NOP was summer > autumn > spring > winter, while that of PDM was summer > autumn > winter > spring. In more than 82% of the NOIs, the NOP/PDM ratio exceeded 40%, and in 26.7% of the events, the ratio

reached above 80%. Consistent with previous studies (Wu et al., 2023), we even observed cases where NOP exceeded PDM, occurring on 75 days (accounting for 12.2% of the total NOIs). Relevant studies have indicated that when nocturnal ozone concentrations exceed 80 μg/m3, there are potential risks to human health and the ecological environment. Taking 80 μg/m^3 as the threshold for hourly ozone concentration [23,31,32], there were 242 days (39.4% of the total NOIs) during the study period when NOP exceeded this threshold, indicating that NOIs in Suizhou cannot be ignored.

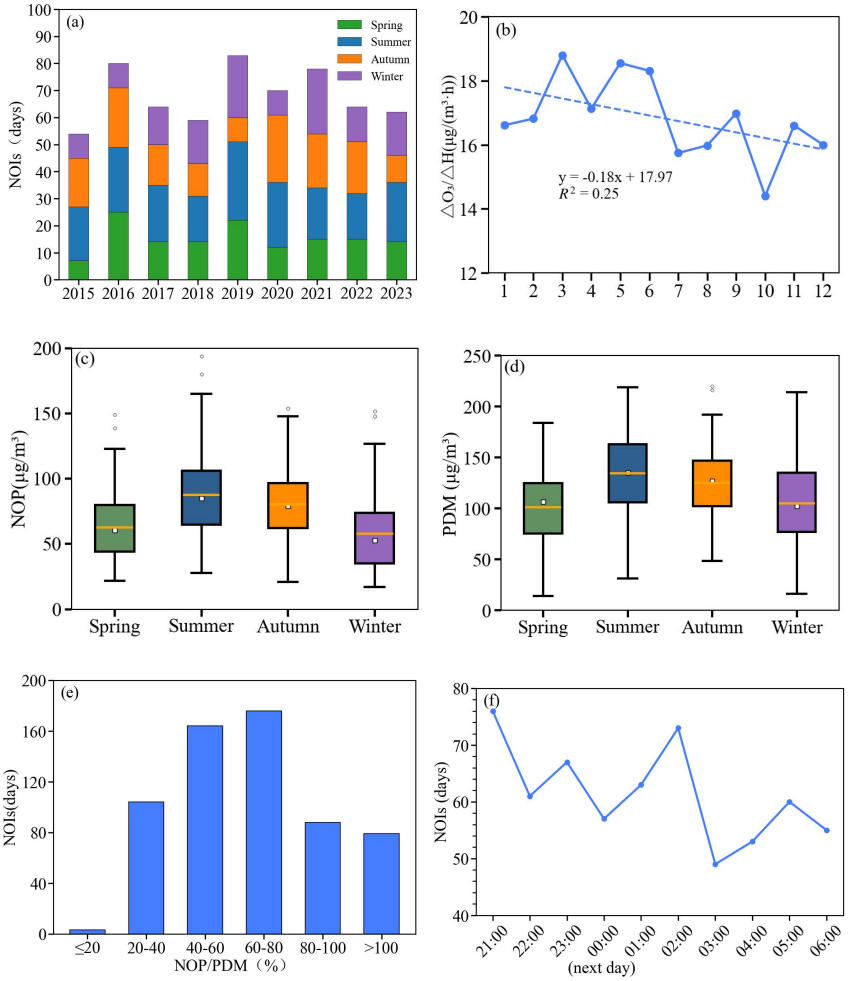

Figure 2. Characteristics of NOIs in Suizhou from 2015 to 2023, Including Annual Frequency (a), Intensity (b), NOP (c), PDM (d), NOP/PDM ratio (e), and diurnal variation of frequency (f)

3.2 Typical case Analysis

3.2.1 Overview of Observations

The NOIs event with the maximum intensity among the 614 samples (20150712_08:00 to 20150715_08:00) was selected as a typical case for analysis. Fig. 3 shows the time series of ozone, NO_2, and CO concentrations at the three national control stations in Suizhou. The figure reveals the following three characteristics: ① NOIs occurred on three consecutive days, all in the late night (01:00 LT on July 13, 01:00 LT on July 14, and 04:00 LT on July 15). ② The event intensity on July 14

reached 57 μg/(m3·h), which was significantly stronger than that on the previous two days and was the maximum among all samples. The NOP on July 14 (105 μg/m3) was markedly higher than that on July 12 (50 μg/m3) and July 13 (41 μg/m3). ③ During the occurrence of NOIs on the first night (July 12) and second night (July 13), surface ozone generally showed an inverse variation with NO_2 and CO. On the third night (July 14), from 03:00 to 04:00 LT on July 15, surface ozone increased while NO_2 and CO decreased simultaneously; however, from 04:00 to 06:00 LT, surface ozone, NO_2, and CO all increased together. Because the intensity was highest on the night of July 14, the following analysis focuses on the causes of the NOIs on that night.

From the hourly variations of surface meteorological elements in Suizhou (figure omitted), the dominant wind direction was northerly during the daytime of July 11–12, shifted to southerly from 14:00 LT on July 12 to 02:00 LT on July 13, with little change in surface pressure and weak surface winds (less than 2 m/s), and variable winds on July 14. During July 11–14, the daily maximum temperatures exceeded 30°C, and relative humidity was low during the daytime, favoring the increase of surface ozone concentration. At night, relative humidity increased significantly, but without solar radiation, ozone could not be produced photochemically and mainly relied on depletion processes. In this study, ozone unexpectedly increased at night, especially on the night of July 14. Additionally, no precipitation occurred at 01:00 LT on July 13 and July 14, but from 04:00 to 06:00 LT on July 15, precipitation intensified at the Chengnan New District, with hourly rainfall amounts of 7.4 mm, 5.6 mm, and 20.6 mm, respectively, corresponding to a sustained increase in ozone concentration. The maximum ozone concentration coincided with the strongest rainfall (06:00 LT), and after 06:00 LT the rainfall weakened and the ozone concentration decreased accordingly.

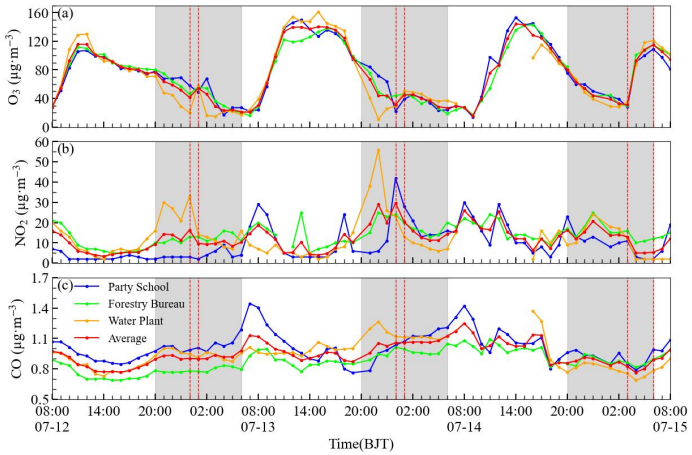

Figure 3. Temporal Variations of O_3, NO_2, and CO during the Typical Case (20150712_08:00-20150715_08:00, BJT) in Suizhou. Shaded Areas Indicate Nighttime (20:00 BJT to 06:00 BJT the next day), and Red Dashed Lines Indicate the Periods of NOIs

3.2.2 Evaluation of Model Simulation Results

Although emission inventories and air quality models have certain uncertainties, the simulation results

still capture the evolution of NOIs in Suizhou. As shown in Fig.4, the observed and simulated surface meteorological variables (temperature, relative humidity, wind speed, and boundary layer height) at the two national stations in Suizhou (Suizhou Station and Guangshui Station) are in good agreement. Four statistical metrics, namely correlation coefficient (R), normalized mean bias (NMB), normalized mean error (NME), and root mean square error (RMSE), were used to validate the simulation results. The results indicate that the model performs well in simulating temperature, relative humidity, and boundary layer height, but shows poorer performance for surface wind speed, possibly due to inherent model errors in handling the surface wind field. The validation results for each meteorological variable are presented in Table 1. Except for the simulation of 10-meter wind speed, which is less satisfactory (low R, high NMB, NME, and RMSE), the other three variables all pass the significance test at the 0.01 level, indicating that the model simulation results are reliable and can be used to evaluate the meteorological conditions and ozone concentration changes during this NOIs event in Suizhou. The simulated surface ozone concentrations are shown in Fig.5. From the spatial distribution, ozone exhibits a pattern of high values in the north and low values in the south. The simulation results generally capture the temporal variation trend of ozone, with a reasonable agreement with the observations. However, there are still limitations in reproducing the exact timing and intensity of the nocturnal ozone increase.

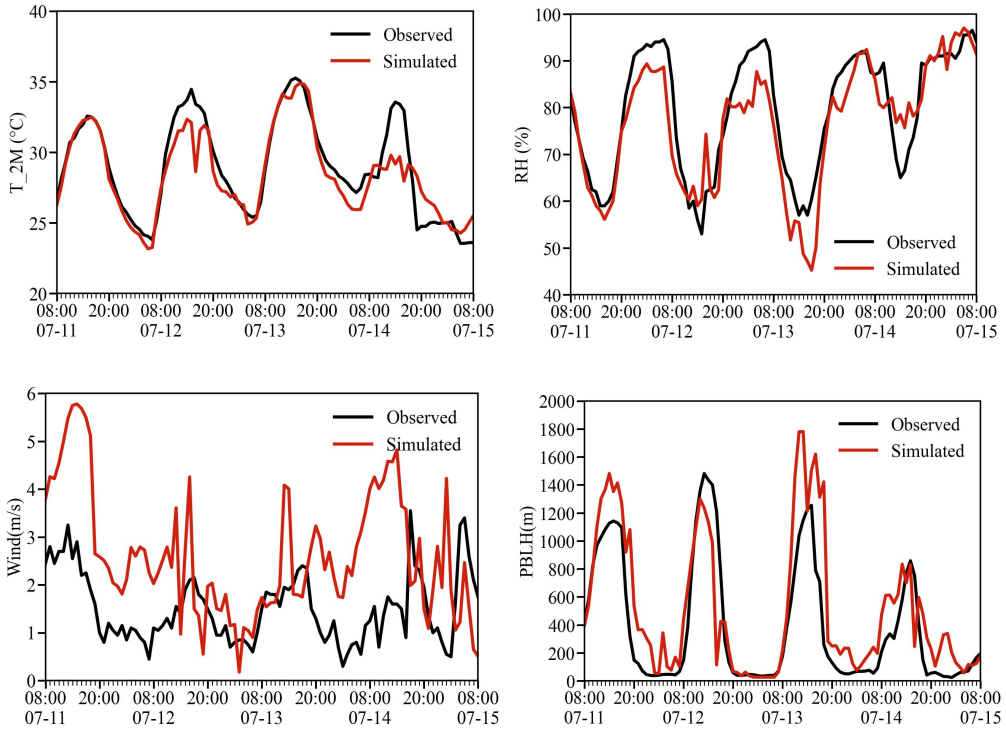

Figure 4. Comparison of Observed (Black Lines) and Simulated (red lines) Time Series of Meteorological Variables during the Typical Case (20150712_08:00-20150715_08:00, BJT) and the Previous Day, Including 2-m Temperature (T_2M), 2-m Relative Humidity (RH_2M), 10-m Wind Speed (Wind_10M), and Planetary Boundary Layer Height (PBLH)

Table 1. Comparison of Observations and Simulations for Meteorological Variables (2-m Temperature (T_2M), 2-m Relative Humidity (RH_2M), 10-m Wind Speed (Wind_10M), and Planetary Boundary Layer Height (PBLH)) at the two National Stations in Suizhou: Suizhou Station (SZ) and Guangshui Station (GS)

	SZ				GS			
	R	NMB(%)	NME(%)	RMSE	R	NMB(%)	NME(%)	RMSE
T_2M	0.92***	1.45	4.10	1.50	0.88***	-4.60	5.42	2.05
RH_2M	0.89***	-11.32	11.85	11.66	0.84***	5.51	8.74	8.23
10M Wind	0.26*	85.28	110.26	1.93	0.21*	64.51	91.83	1.85
PBLH	0.83***	33.56	55.95	309.33	0.79***	33.97	56.88	348.21

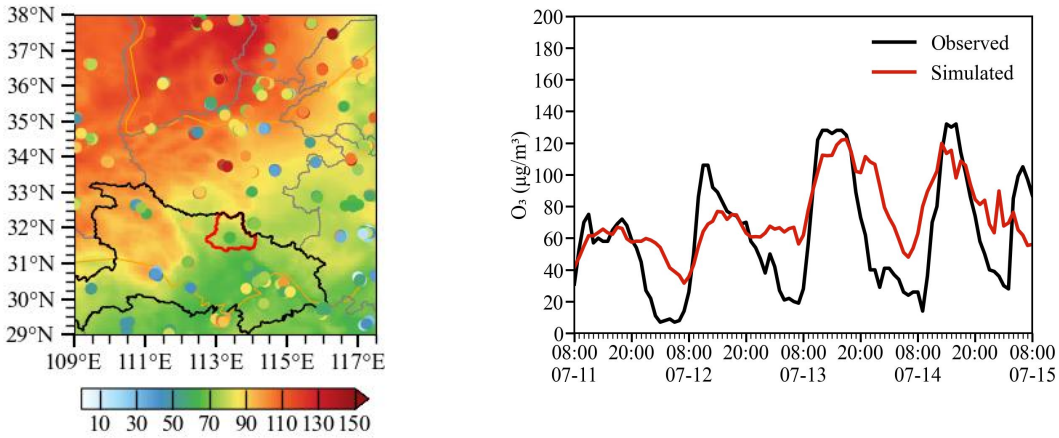

Figure 5. Comparison of Simulated and Observed Ozone Concentrations during the Typical Case (20150712_08:00-20150715_08:00, LT) and the Previous Day. Left panel: Spatial Distribution of Mean Ozone Concentration, with Scatter Points Representing Observations and Colors Representing Simulation Results. Right panel: Time Series of Observed and Simulated Ozone Concentrations

3.2.3 Process Analysis

From the perspective of the large-scale circulation pattern (Fig.6), at 16:40 LT on July 11, 2015, the ninth super typhoon "Chan-hom" made landfall in Zhoushan City, Zhejiang Province, and then turned northeastward. On July 12, the main body of the typhoon moved to the Yellow Sea, while Suizhou, located to its west, was controlled by upper-level northerly winds and experienced clear and fine

weather. On July 13, northerly winds still prevailed during the daytime, with dominant subsidence. The relative humidity at 850 hPa decreased significantly to below 60%. A warm center of 24°C was located at the junction of Shanxi, Henan, and Hebei provinces. The central and western parts of Hubei Province were influenced by a warm trough, forming a warm and dry cap, which further raised the daytime temperature and created a stable stratification that hindered the vertical diffusion of pollutants. As daytime photochemical ozone production proceeded, ozone concentrations at both upper levels and the surface continued to rise on July 13 compared to the previous day (Figs.9), as will be analyzed in further detail below. From the night of July 13 to the daytime of July 14, the region gradually came under weak southerly winds, with slightly increased humidity. Together with the daytime temperature rise, the pseudo-equivalent potential temperature increased (Fig.9), indicating the accumulation of unstable energy. On the night of July 14, the southwesterly warm-moist airflow at 850 hPa intensified significantly, and a quasi-zonal shear line formed between the southerly and easterly winds, markedly enhancing dynamic conditions and favoring the occurrence of precipitation. On July 15, a deep low vortex developed, and Suizhou was located near the center of the vortex, with persistent rainy weather. Combined with the southward intrusion of weak cold air near the surface, the combined effects of wet deposition during the daytime and favorable horizontal diffusion conditions led to a decrease in surface ozone concentrations.

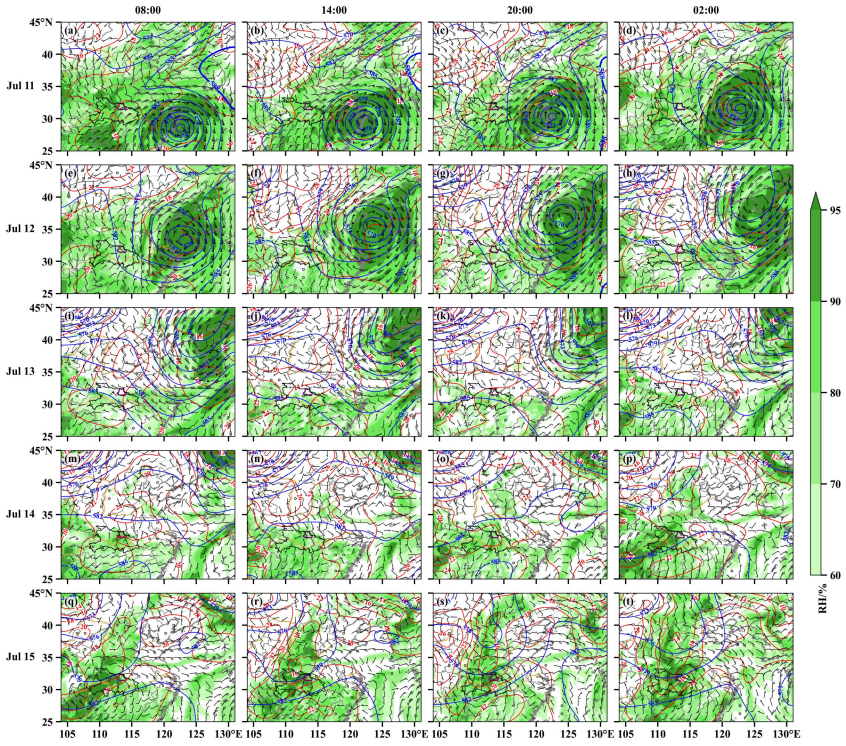

Figure 6. Six-hourly Variations (a-t) of 500 hPa Geopotential Height (blue contours, unit: dagpm), 850 hPa horizontal wind field (wind barbs, unit: m/s), temperature (red contours, unit: °C), and relative humidity (shaded, unit: %) during the typical case (20150712_08:00-20150715_08:00, LT) and the previous day. (The purple solid line indicates the boundary of Suizhou)

Fig.7 shows the surface (10 m) ozone concentration distribution and circulation characteristics during the typical event. Overall, the surface ozone concentration exhibited a clear diurnal variation, with higher values during the daytime (14:00 LT) than at night (02:00 LT and 08:00 LT). At 14:00 LT on July 12, the southern part of North China and the Huanghuai region were controlled by northerly winds on the periphery of the typhoon, with clear and fine weather favorable for photochemical reactions, resulting in ozone concentrations higher than those in the Yangtze-Huaihe region. On the night of July 12, the Huanghuai region maintained relatively high surface ozone concentrations due to northerly wind transport, while the Yangtze-Huaihe region experienced weak winds, and ozone concentrations decreased significantly due to NOx titration and dry deposition. In contrast, urban Suizhou showed a slight increase in nocturnal ozone concentration (figure omitted). As mentioned earlier, the weather pattern during the daytime of July 13 was favorable for rising surface temperatures and sustained photochemical reactions, with ozone concentrations peaking at 14:00 LT; the Jianghan Plain and northeastern Hubei exhibited higher ozone concentrations than Suizhou. On the night of July 13, ozone concentrations decreased significantly over most of Hubei Province. However, due to prevailing southerly winds at the surface and the topographical blocking effect of the Dabie Mountains, ozone continued to accumulate in northeastern Hubei. Under the influence of southerly winds, high-concentration ozone from the Jianghan Plain and northeastern Hubei was transported toward Suizhou, leading to increased ozone concentrations in local areas of Suizhou. For the Suizhou area, daytime ozone concentrations on July 13 and July 14 were significantly higher than those on July 12. On July 14, a surface trough developed over the Hubei-Hunan region. At 14:00 LT, southerly winds prevailed, and the ozone concentration still exhibited a pattern of higher values in southern North China and Hubei compared to the northern part of the region, with eastern Hubei having higher ozone concentrations than the Jianghan Plain. At 20:00 LT, a significant gradient wind formed between the high-pressure system in southern North China and the warm trough over the Yangtze-Huaihe region, and transport processes kept ozone concentrations high in Henan Province. At 02:00 LT on July 15, northerly winds strengthened over the Huanghuai region and extended toward Suizhou, causing ozone accumulation in southern Henan. At the same time, ozone concentrations in the southwestern part of Suizhou were higher than those in the urban area, and the transport by southwesterly winds favored an increase in surface ozone concentration in the urban area.

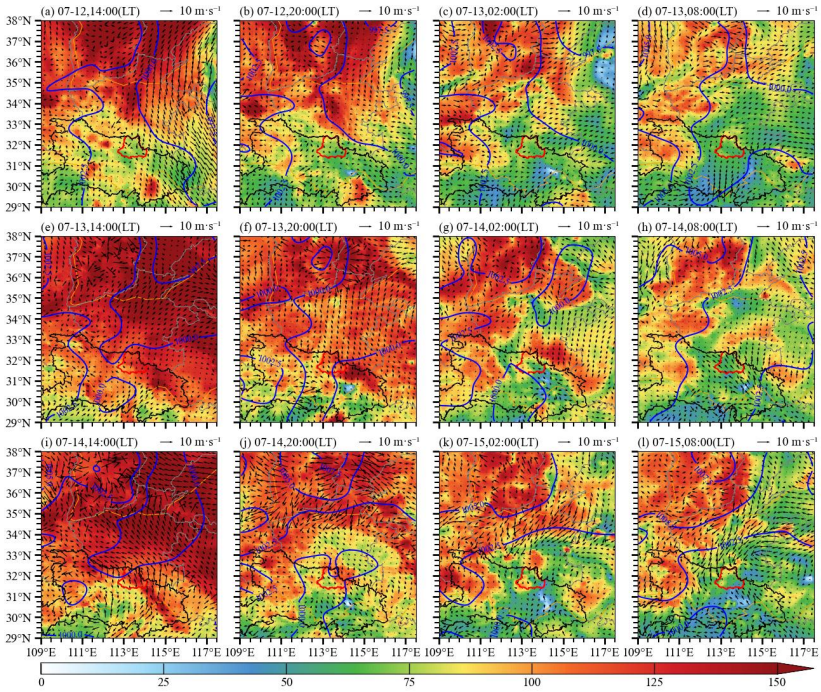

Figure 7. Six-hourly Variations of Surface Sea Level Pressure (Blue Contours, unit: hPa), Horizontal Wind Field (wind barbs, unit: m/s), and Ozone Concentration (shaded, unit: μg/m3) during the Typical Case (20150712_08:00-20150715_08:00, BJT). (The Red Solid Line Indicates the Boundary of Suizhou, and the Black Solid line Indicates the Boundary of Hubei Province)

Fig.8 shows the spatiotemporal distribution characteristics of ozone concentration and circulation patterns at 850 hPa during the typical event. Regarding the variation of ozone concentration, the Henan-Hubei region exhibited a spatial pattern similar to that at the surface, with higher ozone concentrations in the north and lower in the south. On July 12, nighttime ozone concentrations in the Henan-northeastern Hubei area were higher than those during the daytime. Specifically, daytime ozone concentrations in Henan were higher than those in Hubei. Under the influence of northerly wind transport, high-concentration ozone expanded from Henan to northeastern Hubei at night, extending southward to northern Hubei by 08:00 LT on July 13, leading to an increase in ozone concentration at 850 hPa over Suizhou on the night of July 12. In contrast, the diurnal variation of ozone concentration at 850 hPa on July 13–14 was different from that at the surface, with no obvious decrease at night. This is mainly related to the diurnal evolution of the atmospheric boundary layer. In the afternoon, the boundary layer height is relatively high (approximately 1–2 km), gradually decreasing over time. At night, a new stable boundary layer forms, which prevents the downward mixing of ozone from the upper levels. As a result, the high-concentration ozone that accumulated in the mixed layer during the daytime remains above the boundary layer (i.e., at the top of the former mixed layer), forming a relatively stable residual ozone layer. Specifically, at 08:00 LT on July 13, under the control of northerly airflow from the rear of the typhoon, subsidence dominated (as will be further discussed

below), causing an increase in ozone concentration at 850 hPa over Suizhou. At 14:00 LT, the ozone concentration in northeastern Hubei was higher than that in Suizhou, and was transported to Suizhou by southeasterly winds at night, so the nighttime ozone concentration in Suizhou did not decrease. At 14:00 LT on July 14, the southwesterly jet in eastern Hubei and the southeasterly airflow from Anhui-Henan formed a convergence line near the Dabie Mountains, while Suizhou was located in a significant wind divergence zone, favoring the formation of subsidence. At 20:00 LT on July 14, the southwesterly jet in southeastern Hubei pushed northward, and the ozone concentration in Suizhou showed little change compared to that at 14:00 LT. From 02:00 LT on July 15 to 08:00 LT on July 16, a low vortex formed at the junction of Henan and Hubei and moved northeastward, with enhanced dynamic conditions favoring the occurrence of precipitation. During this period, the ozone concentration in eastern Suizhou gradually decreased, while that in western Suizhou showed little change. This may be related to the fact that western Suizhou came under the control of northerly winds behind the shear line instead of southerly winds, transporting high-concentration ozone from Henan to western Suizhou. In addition, previous studies have indicated that there is a relatively stable ozone-rich layer in the middle and lower troposphere (850–500 hPa, 2–6 km), where ozone concentrations generally reach their maximum in summer.

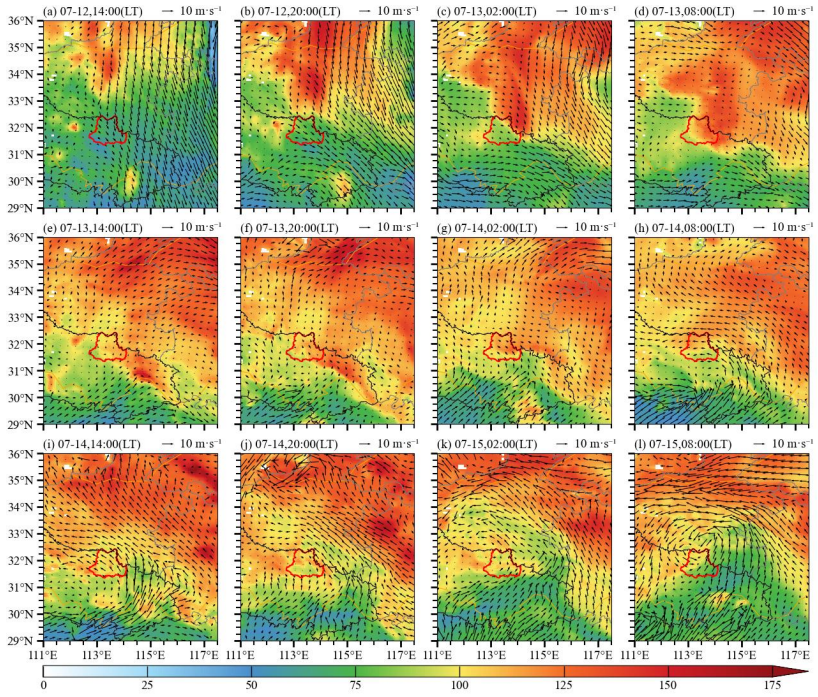

Figure 8. Six-hourly variations of horizontal wind field (wind barbs, unit: m/s) and ozone concentration (shaded, unit: μg/m3) at 850 hPa during the typical case (20150712_08:00-20150715_08:00, LT). (The red solid line indicates the boundary of Suizhou, and the black solid line indicates the boundary of Hubei Province)

A further analysis of the evolution of the typical case is provided below. The station with the highest

NOP during this event (the Shiliqiao Shuichang station) was selected as the representative station. The vertical profiles of ozone concentration, wind profiles, vertical velocity, boundary layer height, friction velocity, K index, pseudo-equivalent potential temperature, and total cloud cover were analyzed, as shown in Fig. 9.

On July 12, the ozone concentration below 850 hPa was uniformly distributed and relatively low. In the middle and upper levels (below 500 hPa), northwesterly winds prevailed with relatively high wind speeds, and subsidence dominated over Suizhou, favoring the downward transport of ozone from the upper levels. This indicates that the increase in ozone concentration at 850 hPa over Suizhou on the night of July 12 was mainly due to subsidence combined with north-to-south transport, while the increase in surface ozone concentration was primarily caused by weak subsidence. During the daytime of July 13, subsidence still dominated in the middle and upper levels, continuing to promote the downward transport of ozone from the ozone-rich layer. On the night of July 13 (20:00–02:00 LT), subsidence occurred at multiple times below 850 hPa, and the residual layer ozone showed a downward expansion trend, providing a prerequisite for the nocturnal ozone increase. On July 12 and 13, the boundary layer height, friction velocity, K index, and pseudo-equivalent potential temperature all exhibited clear diurnal variations (high during the daytime and low at night), indicating that the nighttime atmosphere was more stable than during the daytime. In addition, the daily total cloud cover was relatively low, with predominantly clear and fine weather, favoring photochemical reactions during the daytime and promoting ozone formation.

On July 14, the cloud cover increased compared to the previous two days. The daytime surface temperature was lower than that on the previous two days, with a particularly significant cooling in the afternoon (Fig.9), resulting in a smaller increase in daytime boundary layer height. The ozone concentration in the ozone-rich layer was lower than that on July 13, but still exhibited a diurnal pattern of high during the daytime and low at night. From 14:00 LT on July 14 to 03:00 LT on July 15, ozone within 850 hPa was transported downward under the influence of subsidence, with the intensity of subsidence significantly stronger than that at the same times on July 12–13, favoring further downward transport of residual layer ozone to the surface. Regarding the instability conditions and boundary layer characteristics, from 20:00 LT on July 14 to 08:00 LT on July 15, the K index did not decrease but instead increased to exceed 35°C, indicating that the nighttime atmosphere had an unstable potential, favoring the occurrence of severe convection. From 04:00 to 08:00 LT on July 15, the middle and lower layers became dominated by updrafts, accompanied by precipitation (Fig.9). The boundary layer height and friction velocity increased slightly, indicating enhanced disturbances within the boundary layer. Previous studies have shown that the impact of precipitation on ozone removal after sunset is relatively limited, because wet removal of ozone is indirectly achieved through the removal of HNO_3 and H_2O_2 by water vapor under solar radiation, while heterogeneous processes have little effect on ozone itself [33]. Ozone can remain relatively stable in the residual layer. Therefore, although updrafts and precipitation dominated during 04:00–08:00 LT on July 15, the drag effect of precipitation particles could still

transport ozone from the residual layer downward to the surface. Surface observations show that surface ozone concentration still exhibited a slight increase from 04:00 to 06:00 LT on July 15, while NO_2 and CO concentrations also increased slightly simultaneously. Previous studies have indicated that when regional transport of polluted air masses strengthens, ozone and CO show a positive correlation downwind, whereas when vertical mixing of air masses strengthens, ozone and CO show a negative correlation. During this period, southerly winds prevailed at the surface, suggesting that the increase in surface ozone concentration was also influenced by surface transport. It is worth noting that the model simulation results show that after 04:00 LT on July 15, updrafts dominated in the middle and lower layers, leading to a decreasing trend in ozone concentration below 925 hPa. This discrepancy reflects limitations in the model's representation of vertical motion fields and boundary layer processes, which prevented it from fully reproducing the vertical transport mechanisms of ozone under complex meteorological conditions. Future studies may improve the model parameterization schemes to better simulate such complex nocturnal ozone processes.

In summary, the increase in ozone concentration at 850 hPa over Suizhou on the night of July 12 was mainly caused by subsidence combined with north-to-south transport, while the NOIs on the night of July 12 was mainly caused by weak subsidence. On the nights of July 13 and July 14, the diurnal variation of ozone concentration at 850 hPa was not obvious. The NOIs on the night of July 13 resulted from the combined effects of subsidence and local horizontal transport, with vertical transport playing a greater role than horizontal transport. For the NOIs on the night of July 14, the period from 03:00 to 04:00 LT was dominated by subsidence, while the period from 04:00 to 06:00 LT was governed by the combined effects of local horizontal transport and the drag effect of precipitation particles.

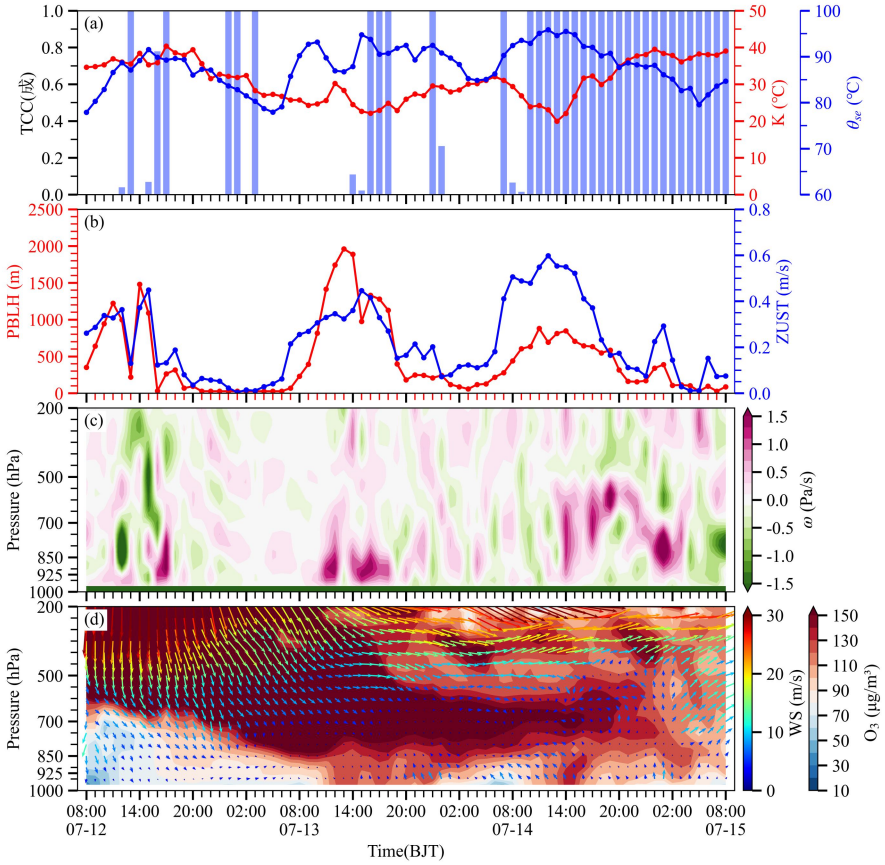

Figure 9. Time series of total cloud cover (unit: tenths), K index (unit: °C), pseudo-equivalent potential temperature (unit: °C) (a); PBLH (unit: m), and friction velocity (ZUST, unit: m/s) (b); vertical velocity (w, unit: Pa/s) (c); and time-vertical cross-section of horizontal wind field (wind barbs, unit: m/s) and ozone concentration (shaded, unit: μg/m3) (d) during the typical case (20150712_08:00-20150715_08:00, LT) in Suizhou

4. Conclusions

Based on surface air pollution observation data, conventional meteorological observation data, and ERA5 reanalysis data in Suizhou from 2015 to 2023, this study systematically analyzed the characteristics of NOIs in Suizhou. The WRF-Chem model was used to simulate the event with the maximum intensity among the 614 NOIs, revealing the impacts of horizontal and vertical transport on the nocturnal increase of surface ozone concentration. The main conclusions are as follows:

(1) A total of 614 NOIs occurred in Suizhou from 2015 to 2023, accounting for 18.7% of the total observation period. Obvious seasonal differences were observed, with summer having the highest frequency, intensity, nocturnal ozone peak (NOP), and peak daytime maximum (PDM), making summer particularly noteworthy. In this study, 26.7% of the NOIs had a NOP/PDM ratio exceeding 80%, and 39.4% of the NOIs had NOP exceeding 80 μg/m3, posing certain potential risks to human health and the ecological environment. Moreover, in 12.2% of the NOIs, NOP exceeded PDM,

indicating that NOIs in Suizhou cannot be ignored.

(2) The NOIs event with the maximum intensity among the 614 events (20150712_08:00 to 20150715_08:00) was selected as the study object. The temporal variation characteristics and large-scale circulation patterns of this case were analyzed based on environmental and meteorological observation data. The WRF-Chem model was used to simulate this event. Evaluation of the model results shows that the WRF-Chem model performs well in simulating the meteorological fields. Except for the 10-m wind speed, the correlation coefficients between the simulated and observed values of the other meteorological variables were all above 0.80, passing the significance test at the 0.01 level. The model captured the spatial distribution and temporal variation of surface ozone concentration reasonably well, but there were still some deviations in reproducing the exact timing and intensity of the nocturnal ozone increase.

(3) The simulation results show that at the surface, the ozone concentration in the Henan-Hubei region exhibited a pattern of high values in the north and low values in the south. Daytime ozone concentrations in Suizhou on July 13 and July 14 were significantly higher than those on July 12, with the wind direction shifting from northerly to southerly. On the night of July 13, influenced by southerly wind transport, a nocturnal ozone increase occurred. At the 850 hPa level, controlled by northwesterly airflow at the rear of the typhoon on July 12, subsidence transported ozone-rich air from the upper levels downward, resulting in higher nighttime ozone concentrations than daytime concentrations at 850 hPa and promoting the increase of surface ozone concentration. On the nights of July 13–14, the nighttime ozone concentrations at 850 hPa showed little difference from the daytime values, but an ozone residual layer existed at night. From 14:00 LT on July 14 to 02:00 LT on July 15, Suizhou was located in a wind divergence zone, and subsidence led to an increase in surface ozone concentration from 03:00 to 04:00 LT on July 15. From 04:00 to 06:00 LT on July 15, the development of the jet stream enhanced disturbances, triggering short-term heavy precipitation. The drag effect of precipitation particles, combined with weak local horizontal transport, jointly led to a sustained increase in nocturnal surface ozone concentration.

References

Wang, Y., Hopke, P. K., Xia, X. et al. (2012). Source apportionment of airborne particulate matter using inorganic and organic species as tracers. *Atmospheric environment*, *55*, 525-532.

An, C., Li, H., Ji, Y. et al. (2024). A review on nocturnal surface ozone enhancement: Characterization, formation causes, and atmospheric chemical effects. *The Science of the total environment*, *921*, 170731-170731.

Brown, S. S., Neuman, J., Ryerson, T. et al. (2006). Nocturnal odd-oxygen budget and its implications for ozone loss in the lower troposphere. *Geophysical research letters*, *33*(8), L08801.

Cheng, N. L., Li, Y. T., Zhang, D. W. et al. (2016). Characteristics of Ozone over Standard and Its Relationships with Meteorological Conditions in Beijing City in 2014. *Environmental Science*, *37*(6), 2041-2051 (in Chinese).

Li, M. H., Gan, Q., Cao, J. et al. (2019). Characteristics of Ozone Pollution and Its Relationship with Meteorological Conditions in Huizhou. *Journal of Tropical Meteorology*, *35*(3), 324-331 (in Chinese).

An, J. L., Wang, Y. S., Li, X. et al. (2007). Analysis of the Relationship between NO, NO_2 and O_3 Concentrations in Beijing. *Environmental Science*, *28*(4), 706-711 (in Chinese).

Wang, Z. S., Li, Y. T., An, X. X. et al. (2018). Variation of O_3 Concentration in Different Regions of Beijing from 2006 to 2015. *Environmental Science*, *39*(1), 1-8 (in Chinese).

Kulkarni, P. S., Bortoli, D., & Silva, A. M. (2015). Reeves C. Enhancements in nocturnal surface ozone at urban sites in the UK. *Environmental Science and Pollution Research*, *22*(24), 20295-20305.

Kalthoff, N., Horlacher, V., Corsmeier, U. et al. (2000). Influence of valley winds on transport and dispersion of airborne pollutants in the Freiburg-Schauinsland area. *Journal of Geophysical Research: Atmospheres*, *105*(D1), 1585-1597.

Zhang, J., Rao, S. T., & Daggupaty, S. M. (1995). Meteorological Processes and Ozone Exceedances in the Northeastern United States during the 12-16 July 1995 Episode. *Journal of Applied Meteorology*, *37*(8), 776-789.

He, C., Lu, X., Wang, H. et al. (2022). The unexpected high frequency of nocturnal surface ozone enhancement events over China: characteristics and mechanisms. *Atmospheric Chemistry and Physics*, *22*(23), 15243-15261.

Feng, Z., Xu, Y., Kobayashi, K. et al. (2022). Ozone pollution threatens the production of major staple crops in East Asia. *Nature Food*, *3*(1), 47-56.

Zhu, L., Han, X., Xu, L. et al. (2024). Nocturnal ozone enhancement in Shandong Province, China, in 2020-2022: Spatiotemporal distribution and formation mechanisms. *Science of the Total Environment*, *925*, 171542.

Lloyd, K. L., Davis, D. D., Marini, R. P., & Decoteau, D. R. (2020). Response of Sensitive and Resistant Snap Bean Genotypes to Nighttime Ozone Concentration. *Journal of the American Society for Horticultural Science*, *145*(6), 331-339.

Kulkarni, P. S., Bortoli, D., & Silva, A. (2013). Nocturnal surface ozone enhancement and trend over urban and suburban sites in Portugal. *Atmospheric environment*, *71*, 251-259.

Yan, X. Y., Gou, X. H., Yang, J. et al. (2020). The Variety of Ozone and its Relationship with Meteorological Conditions in Typical Cities in China. *Plateau Meteorology*, *39*(2), 416-430 (in Chinese).

Yan, W. L., Liu, D. Y., Kang, Z. M. et al. (2019). The characteristics of ozone pollution and its relationship with meteorological factors in Jiangsu. *Journal of the Meteorological Sciences*, *39*(4), 477-487 (in Chinese).

Ye, S., Wang, P., She, Y. Y. et al. (2023). Spatio-temporal variation characteristics and influencing factors of ozone in three major urban agglomerations in China from 2015 to 2020. *Journal of Environmental Engineering Technology*, *13*(4), 1444-1453 (in Chinese).

Zhang, M., Liu, Y., Xu, X. et al. (2025). A Systematic Review on Atmospheric Ozone Pollution in a Typical Peninsula Region of North China: Formation Mechanism, Spatiotemporal Distribution, Source Apportionment, and Health and Ecological Effects. *Current Pollution Reports*, *11*(1), 9.

Li, H., Liu, X., Liu, Z. et al. (2025). Tracking Long-Term Ozone Pollution Dynamics in Chinese Cities with Meteorological and Emission Attribution. *Atmosphere*, *16*(7), 768.

Chen, C., Chen, W., Guo, L. et al. (2025). A comprehensive review of tropospheric background ozone: Definitions, estimation methods, and meta-analysis of its spatiotemporal distribution in China. *Atmospheric Chemistry and Physics*, *25*(21), 15145-15169.

Zhu, X., Ma, Z., Li, Z. et al. (2020). Impacts of meteorological conditions on nocturnal surface ozone enhancement during the summertime in Beijing. *Atmospheric Environment*, *225*(D20), 117368.

Wu, Y., Chen, W., You, Y. et al. (2023). Quantitative impacts of vertical transport on the long-term trend of nocturnal ozone increase over the Pearl River Delta region during 2006-2019. *Atmospheric Chemistry and Physics*, *23*(1), 453-469.

Chen, N., Liu, C. H., Xu, K. et al. (2020). EOF/SVD Based Characteristics of Ozone in Hubei Province in 2018 and the Relationship Between Its High Values and Meteorological Factors. *Environmental Monitoring in China*, *36*(2), 88-95 (in Chinese).

Chen, N., Lu, X. C., Yao, T. et al. (2017). Ozone Distribution Characteristics and Its Control Measures in Hubei. *Environmental Monitoring in China*, *33*(4), 150-158 (in Chinese).

Yang, C. M., Huang, Y., Huang, H. B. et al. (2025). Sensitivity analysis of O_3 generation in Hubei Province based on TROPOMI data. *China Environmental Science*, *45*(1), 50-57 (in Chinese).

Xu, P., Xie, Z., Zhao, Y. et al. (2025). Estimation of High-Spatial-Resolution Near-Surface Ozone over Hubei Province. *Atmosphere*, *16*(7), 786.

Wu, Q., Liu, D., Zhu, K. G. et al. (2024). Characteristics of ozone pollution and its relationship with meteorological factors in Hubei Province from 2018 to 2022. *Acta Scientiae Circumstantiae*, *44*(10), 42-51 (in Chinese).

Zhang, Q. Q., & Zhang, X. Y. (2019). Ozone Spatial-temporal Distribution and Trend over China Since 2013: Insight from Satellite and Surface Observation. *Environmental Science*, *40*(3), 1132-1142 (in Chinese).